British Columbia's (western Canada) induced earthquake focal mechanisms

Sahar Behzadi[1], Noorbakhsh Mirzaei[2], Javad Kazemian[3], Alireza Babaie Mahani[4]

[1] *M.Sc., Institute of Geophysics, University of Tehran, Tehran, Iran. sbehzady1373@gmail.com*

[2] *Professor, Institute of Geophysics, University of Tehran, Tehran, Iran. nmirzaii@ut.ac.ir*

[3] *Postdoctoral Associate, Dept. of Earth Sciences, University of Western Ontario, jkazemia@uwo.ca*

[4] *Director at Mahan Geophysical Consulting Inc, ali.mahani@mahangeo.com*

ABSTRACT

Earthquakes caused by human activities have been documented in many regions worldwide. Since industrial activities could trigger earthquakes, the topic of induced earthquakes has embraced a great deal of scientific interest in recent years. There are indications to link the fluid injection/extraction to several damaging events (i.e., Mw > 5) in different parts of the Earth. However, recognizing those events in naturally elevated seismic areas is challenging. Estimating the source parameters for induced earthquakes reveals essential properties of their nature and can improve the findings about the dynamics and tectonics of such events. In this study, we determined the parameters of the Eikonal model for eight more significant induced earthquakes in the Western Canada Sedimentary Basin (WCSB) using the KIWI tool. These events occurred from August 2014 to March 2019 with a moment magnitude range of 3.7 to 4.4 and relatively low depths associated with the energy activities like hydraulic fracturing (HF) operations in the area. We performed the Inversion process in three steps to determine the source parameters, including eight parameters related to the point source and five parameters of the extended source. We aim to evaluate the parameters for creating a robust and reliable inversion in both the frequency and time domains. Results show that the depths of chosen earthquakes are shallower than the depths of specific seismic events in the area. Results of the inversion process for the 2014/08/04, 2014/08/09, 2015/06/13, 2015/08/17, and 2018/11/30 events revealed a compressional focal mechanism on planes striking northwest-southeast. This solution is compatible with the orientation and mechanism of pre-existing faults in the Rocky Mountain fold-and-thrust belt. The 2014/04/03, 2016/01/12, and 2019/03/04 events revealed left-lateral strike-slip focal mechanisms, which are well-matched with the slip mechanism in central Alberta.

Keywords: Induced Earthquake, Earthquake Focal Mechanisms, Hydraulic Fracturing, Inversion Process, Eikonal model.

INTRODUCTION

Hundreds of earthquake clusters have been linked to various industrial activities involving fluid injection/extraction or material removal from the underground (Foulger et al. 2017; Grigoli et al. 2017). In the United States and Canada, oil and gas-producing activities are the dominant factors for such induced seismicity (Ellsworth, 2013; Atkinson et al., 2016). Several Mw>5 earthquakes in the United States (e.g. McGarr 2014) have been identified as induced seismicity. Since 2013, multistage HF operations, which require drilling horizontal wells and injection of fluid mixture underground, have been widely utilized in the WCSB (e.g., Atkinson et al., 2016; Wang et al., 2016). Most HF-induced earthquakes occurred on Montney and Duvernay, which has been suggested to be associated with their over-pressured nature (Eaton and Schultz 2018). Both formations are organic-rich and have hundreds of multistage HF wells operated by various oil companies. For induced seismicity in western Canada, hydraulic fracturing is mainly responsible for the increasing number of intraplate earthquakes.

However, induced clusters indicate unique behavior among thousands of injection wells in the WCSB. They have significant spatial and temporal variations and swarm-like behavior that may not follow recurrence laws, for example, fore-shock and after-shock patterns with dominant main

shock (Skoumal et al., 2015). This particular behavior and many other causes (unusual depth range and non-DC component) separate natural earthquakes from induced ones.

The active deformation of the foreland basin of the WSCB is controlled by thrust faulting throughout the Canadian-Cordillera. This fault system is likely related to deeper structures, even within the basement. The world stress map of Heidbach et al. (2016) indicates NE-striking of the maximum horizontal stress axis in this area. The sedimentary layer thickness is estimated from the surface of the Canadian Shield in the east to 6 km beneath the Rocky Mountains in the west (Hope et al., 1999). Moreover, this region's oil and gas reservoirs were located at depths up to 4 km (Green and Mountjoy 2005). Seismicity in the WCSB mainly consists of three kinds of sources: mining blasts, natural earthquakes, and induced earthquakes (Figure 1A). The broadband seismic monitoring in Alberta, the central part of the WCSB, primarily relies on five seismic networks: CRANE (Canadian Rockies and Alberta Network), RAVEN (Regional Observatory of Alberta Earthquake Network), TD (TransAlta Dam Monitoring Network), CNSN (Canadian National Seismograph Network), and NEBC (Northeast British Columbia Seismographic Network) (Figure 1B). The combination of networks provides relatively uniform coverage throughout Alberta and British Colombia. In recent years, expanding broadband seismic networks have provided valuable data that make moment tensor inversion possible for the Mw~4 earthquakes. In this project, the parameters of the Eikonal model for eight more significant induced earthquakes were determined using the KIWI tool. These events occurred from August 2014 to March 2019 with a moment magnitude range of 3.7 to 4.4 and relatively low depths associated with the energy activities like hydraulic fracturing operations in the WCSB.

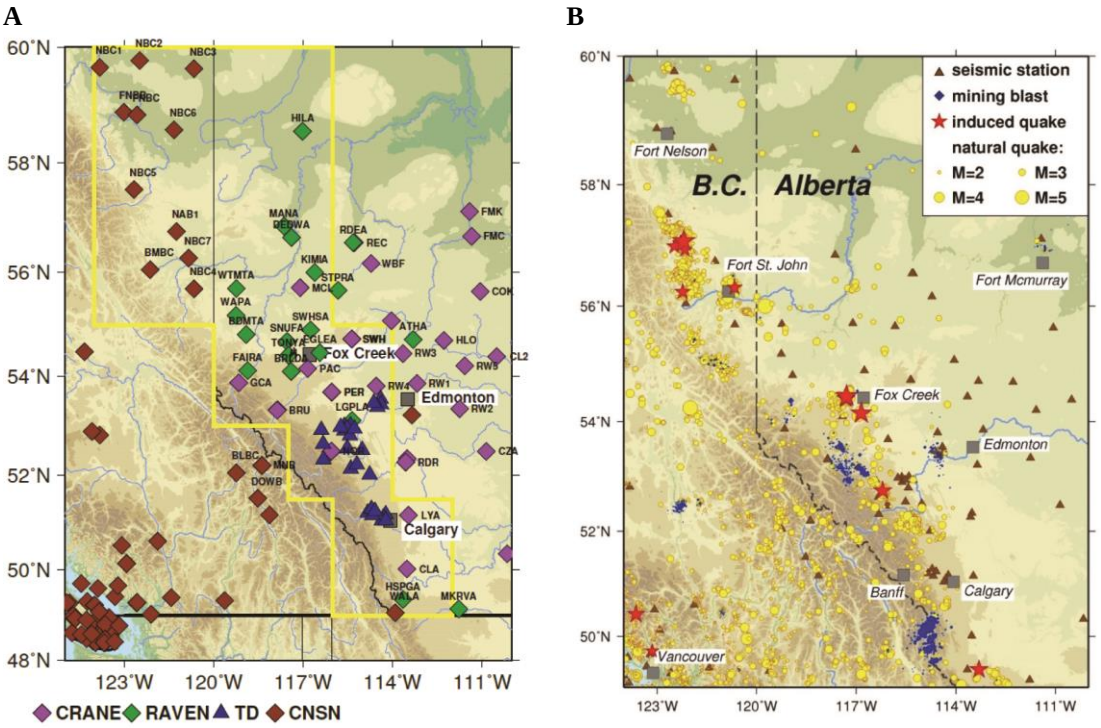

Figure 1: A) Seismic networks in the study area. The active seismic region of WCSB is roughly defined by the yellow box, following Zhang et al. (2016). Data used in this study are obtained from 5 seismic networks: CRANE, RAVEN, TD, CNSN, and NEBC (plotted using the same symbol as CNSN stations). B) Distribution of earthquakes (1985-2017, yellow circles), mining blasts (blue diamonds), and seismic stations (brown triangles) in the WCSB. The red stars mark significant induced earthquakes.

METHODOLOGY AND DATA

KInematic Waveform Inversion (KIWI) is an inversion tool to perform iterative moment tensor inversion for the point and extended source parameters in regional distances (Heimann et al.,

2019). Three inversion steps in the time and frequency domains are used in consecutive processes to evaluate kinematic source parameters in the KIWI tool. The point source and radiation pattern (fault plain parameters, scalar moment, and centroid depth) inversions are the method's steps. Moreover, the KIWI for earthquakes with Mw>5.5 can use more physical information about earthquakes.

We set up the inversion to fit 3-component full displacement waveforms simultaneously in the time and frequency domains. Synthetic seismograms were computed using pre-calculated green's functions based on a regional velocity model.

RESULTS

We applied the method on all seismic networks (CRANE, RAVEN, TD, CNSN, and NEBC) datasets in the WCSB from August 2014 to March 2019, with a moment magnitude range of 3.7 to 4.4. These datasets have great seismic station coverage of events, which made our results have good reliability. The eight focal mechanisms in this study in the WCSB are divided into two main categories; 1. N-S or E-W striking strike-slip focal mechanisms (in central Alberta), 2. NW striking almost pure compressional focal mechanisms (in the Rocky Mountains). The results of the 2018/11/30 event (M_w = 4.4) with 3.3 km depth as a sample of these operations are shown in Figure 2.

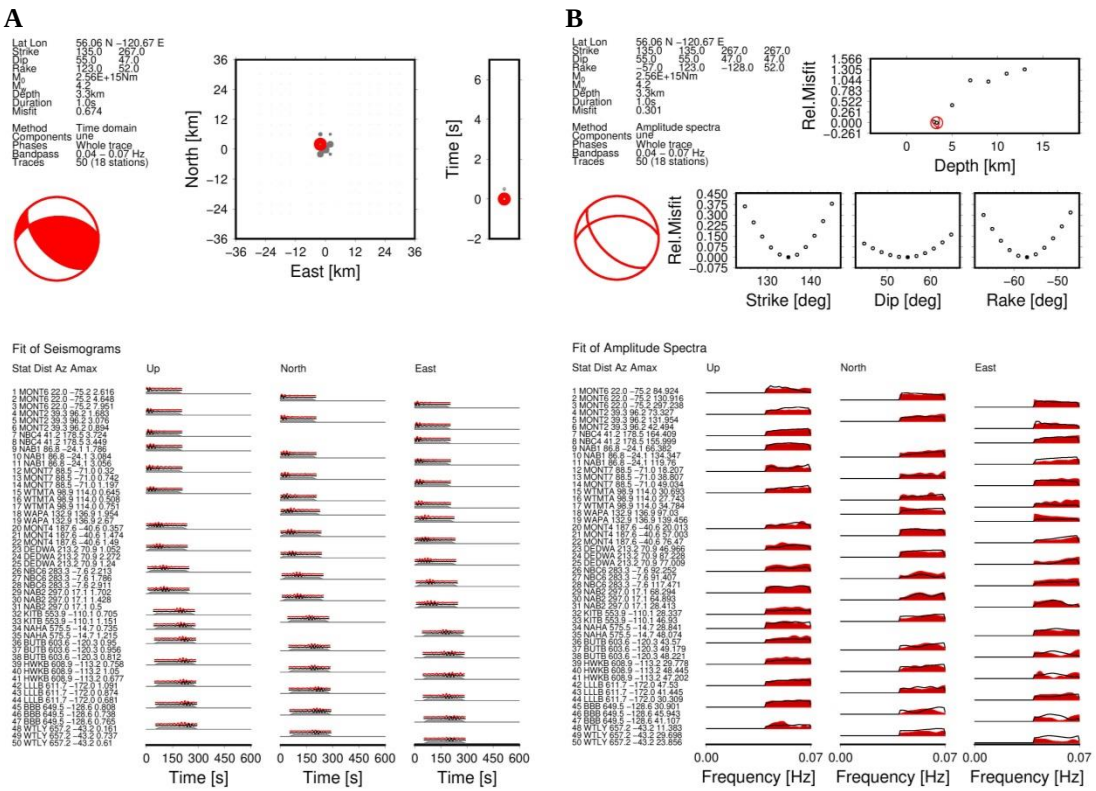

C

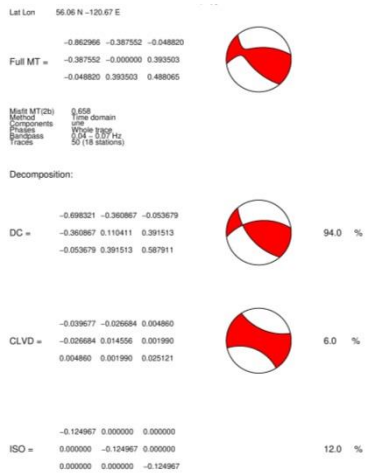

Figure 2: The results of the KIWI inversion tool for the 2018/11-30 event.
A) The focal mechanism and the event's best location and origin time. Also, the A quality waveform fittings of the inversion result in the time domain (The red bands are observed, and the black ones are synthetics).
B) The focal mechanism, and the best fit for depth, strike, dip and rake. Also, the A quality waveform fittings of the inversion result in the frequency domain (The red bands are observed, and the black ones are synthetics).
C) The full moment tensor parameters. In addition, the decomposition of moment tensor components to DC, CLVD, and ISO.

CONCLUSION

Revealing the tie between HF operation and anthropogenic earthquakes helps optimize hazard assessment costs all over the world's seismic regions. The exceeding rate of induced earthquakes in the WCSB by industrial gas explorations makes this region an important hazardous area. The results of this study would be helpful in hazard assessment such as this region. The induced focal mechanisms obtained in this study are located in an area that is poor in natural earthquakes. Interestingly, these induced focal mechanisms are similar to natural earthquake focal mechanisms. They are in good agreement with the maximum horizontal stress of the region. However, the focal mechanisms are scattered through the Rocky Mountains (the area of gas extraction and fluid injection) and follow the principal stress axis of the area.

REFERENCES

Atkinson, G.M., Eaton, D.W., Ghofrani, H., Walker, D., Cheadle, B., Schultz, R., Shcherbakov, R., Tiampo, K., Gu, J., Harrington, R.M. and Liu, Y., 2016. Hydraulic fracturing and seismicity in the Western Canada Sedimentary Basin. Seismological research letters, 87(3), pp. 631-647.

Eaton, D.W. and Schultz, R., 2018. Increased likelihood of induced seismicity in highly overpressured shale formations. Geophysical Journal International, 214(1), pp. 751-757.

Ellsworth, W.L., Injection-Induced Earthquakes', 2013. Science, 341(6142.(

Foulger, G.R., Wilson, M.P., Gluyas, J.G., Julian, B.R. and Davies, R.J., 2018. Global review of human-induced earthquakes. Earth-Science Reviews, 178, pp. 438-514.

Green, D.G. and Mountjoy, E.W., 2005. Fault and conduit controlled burial dolomitization of the Devonian west-central Alberta Deep Basin. Bulletin of Canadian Petroleum Geology, 53(2), pp. 101-129.

Grigoli, F., Cesca, S., Priolo, E., Rinaldi, A.P., Clinton, J.F., Stabile, T.A., Dost, B., Fernandez, M.G., Wiemer, S. and Dahm, T., 2017. Current challenges in monitoring, discrimination, and management of induced seismicity related to underground industrial activities: A European perspective. Reviews of Geophysics, 55(2), pp. 310-340.

Heidbach, O., Rajabi, M., Cui, X., Fuchs, K., Müller, B., Reinecker, J., Reiter, K., Tingay, M., Wenzel, F., Xie, F. and Ziegler, M.O., 2018. The World Stress Map database release 2016: Crustal stress pattern across scales. Tectonophysics, 744, pp. 484-498.

Heimann, S., Vasyura-Bathke, H., Sudhaus, H., Isken, M.P., Kriegerowski, M., Steinberg, A. and Dahm, T., 2019. A Python framework for efficient use of pre-computed Green's functions in seismological and other physical forward and inverse source problems. Solid Earth, 10(6), pp.

1921-1935.

Hope, J., Eaton, D.W. and Ross, G.M., 1999. Lithoprobe seismic transect of the Alberta Basin: Compilation and overview. Bulletin of Canadian Petroleum Geology, 47(4), pp. 331-345.

McGarr, A., 2014. Maximum magnitude earthquakes induced by fluid injection. Journal of Geophysical Research: solid Earth, 119(2), pp. 1008-1019.

Wang, R., Gu, Y.J., Schultz, R., Kim, A. and Atkinson, G., 2016. Source analysis of a potential hydraulic-fracturing-induced earthquake near Fox Creek, Alberta. Geophysical Research Letters, 43(2), pp. 564-573.

Skoumal, R.J., Brudzinski, M.R. and Currie, B.S., 2015. Distinguishing induced seismicity from natural seismicity in Ohio: Demonstrating the utility of waveform template matching. Journal of Geophysical Research: Solid Earth, 120(9), pp. 6284-6296.